Study of Skin Friction in Channels by Lattice Boltzmann Method

A. Zarghami*
Department of Engineering,
Science and Research Branch, Islamic Azad University, Fars, Iran
E-mail: a.zarghami@fsriau.ac.ir
*Corresponding author

N. Ahmadi
Department of Engineering,
Science and Research Branch, Islamic Azad University, Fars, Iran
E-mail: negar.ahmadi670@gmail.com

Received: 12 May 2012, Revised: 12 September 2012, Accepted: 3 December 2012

Abstract: A finite volume-lattice Boltzmann algorithm is applied to study skin friction behaviour in different channel flows. For this purpose, cell centred scheme is adapted to discretize the Boltzmann equation and consistent boundary conditions are also addressed, which resulted in a wider domain of stability. A simulation of flow in a two dimensional channels with different geometries are carried out. The results are compared with previous valid results in which favourable agreement was observed. The results showed that skin friction in plane Poiseuille flow converged to 24/Re, but skin friction distribution in suddenly enlarged channels regain symmetry after some distance downstream of the expansion plane.

Keywords: Channel Flow, Lattice Boltzmann Method, Skin Friction, Recirculation Region

Reference: Zarghami, A., and Ahmadi, N., "Study of Skin Friction in Channels by Lattice Boltzmann Method", Int J of Advanced Design and Manufacturing Technology, Vol. 6/ No. 3, 2013, pp. 91-98.

Biographical notes: A. Zarghami received his PhD in Mechanical Engineering – Energy Conversion from Shahrood University of Technology, Shahrood, Iran, in 2012. He is currently Assistant Professor at the Department of Engineering, Science and Research Branch, Islamic Azad University, Fars, Iran. His research interest includes Fluid Mechanics, Lattice Boltzmann Method and CFD. **N. Ahmadi** is a graduate student of Computer Engineering – AI and Robotics, Iran University of Science and Technology. Her main research focuses on application of different AI tools in engineering.

1 INTRODUCTION

The lattice Boltzmann method (LBM) serves as an alternative to Navier–Stokes equations. From its birth over 20 years ago, LBM have been used successfully in simulating the various flows. The obvious advantages of using LBM are the simplicity of programming, the parallelism of the algorithm and the capability of incorporating complex microscopic interactions [1]. As a different approach from the conventional computational fluid dynamics, the LBM has been demonstrated to be successful in simulations of complex fluid flows [2].

The fundamental philosophy of the lattice Boltzmann equation (LBE) is to construct simple models based on kinetic theory that preserve the conservation laws and necessary symmetries such that the emerging behavior of these models obeys the desired macroscopic equations. The kinetic nature of the LBM leads to the following features that distinguish the LBM method from any other conventional CFD method. First, the convection operator of the LBE model is linear in phase space, similar to that of the Boltzmann kinetic equation but different than the Euler or the Navier-Stokes equations. Second, the pressure is obtained through an equation of state, as opposed to solving a Poisson equation in the incompressible Navier-Stokes equations. Third, with the Navier-Stokes equations, the constitutive relations are input from empirical data, while with the LBE method, the constitutive relations emerge as a result of proper modelling of inter-particle potentials. Fourth, unlike the Navier-Stokes or Euler equations, in which macroscopic conservation laws are discretized, the LBM utilize a set of discrete particle velocities such that the conserved quantities are preserved up to machine accuracy in the calculations. Several references are available to obtain an entry to the theory and methodology of LBE [2], [3].

In LBM, the physical spatial structure of the lattice is intrinsically coupled to the velocity discretization of particle distribution function. The advantage is the Lagrangian, exact treatment of advective transport, and hence, a zero numerical diffusion. On the other hand, straightforward integration of the LBE on a structured or unstructured mesh is not possible. This leads to difficulty in adapting the mesh to complex flow-structures such as separation, vortices, shears flows and boundary layers etc., and to satisfy boundary conditions on irregular geometries [4]. Such difficulty may be overcome by decoupling the numerical mesh from the lattice structure, and taking recourse to, one of finite difference, finite element or finite volume approaches [5-7]. But the finite volume approach is gaining popularity owing to their robustness and flexibility to handle complex flow domains.

In this paper, we will consider a finite-volume formulation of LBM for study skin friction distribution in channel flows. A cell-centered approach is used for space discretization and consistent boundary conditions are also addressed. The performance of the formulation is systematically investigated by simulating plane Poiseuille flow and suddenly enlarged channel flow. For each of these flows, the present scheme is validated with the literature results.

2 FINITE VOLUME FORMULATION OF LBM

The lattice Boltzmann equation (LBE) can be directly derived from the Boltzmann equation by discretization in phase space without borrowing the concept of particles jumping from site to site as in the LGA model [4]. The commonly used LBM models can be regarded as specific discretizations of the LBE on regular lattices. The flexibility gained in unlocking the spatial and velocity lattices from each other provides us in designing our cell centered finite-volume scheme. A popular kinetic model is the single relaxation time approximation, the so-called Bhatnagar–Gross–Krook (BGK) model [8].

$$\frac{\partial f_i}{\partial t} + \vec{v}_i.\nabla f_i = -\frac{1}{\tau}\left(f_i - f_i^{eq}\right) \qquad i = 1,...,n \tag{1}$$

where n is the number of different velocities in the model, f^{eq} is the particle equilibrium distribution function associated with motion along the i^{th} direction in velocity space, $\vec{v}_i$ the velocity in the i^{th} direction, τ is the relaxation time and the right hand side of the equation is the collision operator.

In the LBM, only a small set of discrete velocities are used to approximate the Boltzmann kinetics of the continuum velocity. So, to solve for f numerically, equation (1) is first discretized in the phase space using a finite set of velocities without violating the conservation laws. For 2D flows, the nine velocity model denoted as the D_2Q_9 model, has been widely used. The discrete velocities are given by $\vec{v}_0 = 0$ and $\vec{v}_i = \lambda_i(\cos\theta_i, \sin\theta_i)$ with $\lambda_i = 1, \theta_i = (i-1)\pi/2$ for i=1~4 and $\lambda_i = \sqrt{2}, \theta_i = (i-5)\pi/2 + \pi/4$ for i=5~8 (see Fig. 1). The macroscopic density ρ and velocity **u** are determined by $\rho = \sum_i f_i$ and $\rho\mathbf{u} = \sum_i f_i\vec{v}_i$ respectively. The macroscopic pressure is given by equation of state of an ideal gas as $p = c_s^2\rho$ and the corresponding kinematic shear viscosity is related to the relaxation time by $\nu = c_s^2\tau$ [9].

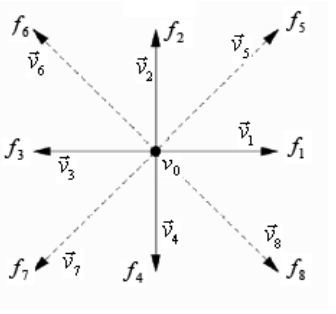

Fig. 1 Discrete velocity vectors of D_2Q_9 model

The equilibrium distribution for D_2Q_9 model is defined by:

$$f_i^{eq}(\vec{x},t) = w_i\rho\left[c_1 + c_2(\vec{v}_i.\mathbf{u}) + c_3(\vec{v}_i.\mathbf{u})^2 + c_4(\mathbf{u}.\mathbf{u})\right] \quad (2)$$

where $c_1 = 1, c_2 = 1/c_s^2, c_3 = 1/(2c_s^4), c_4 = -1/2c_s^2$ and $c_s = c/\sqrt{3}$ is the speed of sound in the lattice. w_i is the weighting factor and equals 4/9 for i=0, 1/9 for i=1~4 and 1/36 for i=5~8.

Now we choose 2D unstructured rectangular meshes to illustrate how the cell centered FV scheme is constructed. Fig. 2 shows a generic situation in which quadrilateral meshes surround an arbitrary cell. The scheme we report here is a cell-centered finite volume method.

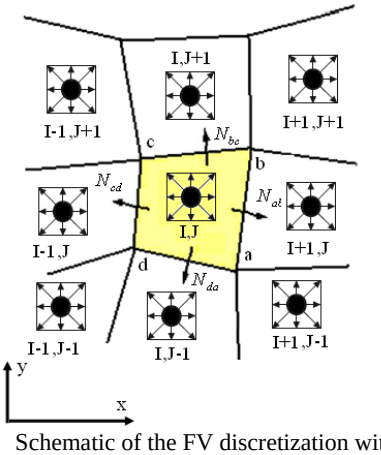

Fig. 2 Schematic of the FV discretization with cell-centered lattice

The integration of the first term in equation (1) is approximated as:

$$\int_{abcd}\frac{\partial f_i}{\partial t}dA \approx \left[\frac{\partial f_i}{\partial t}\right]_{I,J}.A_{I,J} \quad (3)$$

Where $A_{I,J}$ is the area of *abcd*. In the above equation, we have made an approximation that f_i is constant over the area *abcd* to avoid having to solve a set of equations. This is a common practice in the finite volume methods. By using the Divergence theorem and upwind scheme, integration of the second term of equation (1) will give fluxes though the four edges *ab*, *bc*, *cd*, and *da* [10].

$$\int_{abcd} v_i.\nabla f_i\,dA = \int_{abcd}\left[\frac{\partial(\vec{v}_{ix}\cdot f_i)}{\partial x} + \frac{\partial(\vec{v}_{iy}\cdot f_i)}{\partial y}\right]dxdy =$$
$$\begin{cases}[f_i]_{I,J}\,v_i.N_{ab} & if\ v_i.N_{ab} \ge 0\\ [f_i]_{I+1,J}\,v_i.N_{ab} & if\ v_i.N_{ab} < 0\end{cases} + \begin{cases}[f_i]_{I,J}\,v_i.N_{bc} & if\ v_i.N_{bc} \ge 0\\ [f_i]_{I,J+1}\,v_i.N_{bc} & if\ v_i.N_{bc} < 0\end{cases}$$
$$+\begin{cases}[f_i]_{I,J}\,v_i.N_{cd} & if\ v_i.N_{cd} \ge 0\\ [f_i]_{I-1,J}\,v_i.N_{cd} & if\ v_i.N_{cd} < 0\end{cases} + \begin{cases}[f_i]_{I,J}\,v_i.N_{da} & if\ v_i.N_{da} \ge 0\\ [f_i]_{I,J-1}\,v_i.N_{da} & if\ v_i.N_{da} < 0\end{cases}$$
$$\approx \sum_k \vec{v}_i\cdot N_k(f_i)_k \quad (4)$$

Where $N_k = (\Delta yi - \Delta xj)_k$ and $k = ab, bc, cd, da$. Assuming the linearity of f_i, f_i^{eq} over each internal cell, the integration over the collision term of equation (1) results in the following formula:

$$-\int_{abcd}\frac{1}{\tau}(f_i - f_i^{eq})dA = -\frac{A_{I,J}}{\tau}\left[\frac{1}{4}[\Delta f_i]_{I,J} + \right.$$
$$\frac{1}{8}\left\{[\Delta f_i]_{I+1,J} + [\Delta f_i]_{I,J+1} + [\Delta f_i]_{I-1,J} + [\Delta f_i]_{I,J-1}\right\} +$$
$$\left.\frac{1}{16}\left\{[\Delta f_i]_{I+1,J-1} + [\Delta f_i]_{I+1,J+1} + [\Delta f_i]_{I-1,J+1} + [\Delta f_i]_{I-1,J-1}\right\}\right] \quad (5)$$

Where $\Delta f_i = f_i - f_i^{eq}$. Note that the integration of the collision terms in boundary cells takes the following form:

$$-\int_{abcd}\frac{1}{\tau}(f_i - f_i^{eq})dA = -\frac{A_{I,J}}{\tau}\left[(f_i)_{I,J} - (f_i^{eq})_{I,J}\right] \quad (6)$$

A modified fifth order, Runge-Kutta scheme is used to advance the f_i in time. This scheme can be applied as follows:

$$f_i^{n+1} = f_i^n + \alpha_k\Delta f_i^{k-1} \quad (7)$$
$$\therefore \alpha_1 = 0.0695, \alpha_2 = 0.1602, \alpha_3 = 0.2898, \alpha_4 = 0.5, \alpha_5 = 1$$

Where k=1,…,5 and n denote the time step. Therefore:

$$\Delta f_i^{k-1} = \Delta t Q_i^{k-1}/A_{I,J} \quad (8)$$

Where $Q_i^{k-1} = \sum\left(f_i^{k-1}\right)_{Collisions} - \sum\left(f_i^{k-1}\right)_{Fluxes}$. Thus the new-time particle distribution function is calculated as follows:

$$f_i^{n+1} = f_i^n + \alpha_k \frac{\Delta t}{A_{I,J}}\left[\sum\left(f_i^{k-1}\right)_{Collisions} - \sum\left(f_i^{k-1}\right)_{Fluxes}\right] \quad (9)$$

The time step based on the CFL (Courant–Friedrichs–Lewy) criterion is given by:

$$\Delta t = CFL \times \frac{\mathrm{Min}\left(\sqrt{\Delta x_{I,J}^2 + \Delta y_{I,J}^2}\right)}{\mathrm{Max}\left(\sqrt{u_{I,J}^2 + v_{I,J}^2}\right)} \quad (10)$$

Where the term CFL is set to less than 0.7 for more stability and $\Delta x_{I,J}, \Delta y_{I,J}$ are the projected lengths of the minimal area cell on the *x* and *y* directions respectively.

3 BOUNDARY CONDITIONS

In order to transform hydrodynamic boundary conditions to the boundary conditions for the distribution functions, additional lattices at the edge of each boundary cell are introduced. Then, boundary nodes are treated like internal nodes, except that the fluxes over boundary edges also have to be evaluated [11]. As indicated in Fig. 3, physical boundaries of the computational domain are defined to be aligned with the lattice grid lines. The *inlet* boundary conditions at $I = 1$ are given by:

$$\begin{aligned} &f_1 = f_3 + 2u_{in}/3 \;\;,\;\; f_5 = f_7 + 0.5\left(f_4 - f_2\right) + u_{in}/6 \\ &f_8 = f_6 + 0.5\left(f_2 - f_4\right) + u_{in}/6 \end{aligned} \quad (11)$$

At the *outlet* boundary i.e. $I = N_x$, the unknown distribution functions are extrapolated as follows:

$$\begin{aligned} &f_i\left(I = N_x, J\right) = \\ &1.5 f_i\left(I = N_x - 1, J\right) - 0.5 f_i\left(I = N_x - 2, J\right) \end{aligned} \quad (12)$$

The above described scheme is also known as Zou and He boundary conditions, suggesting the name of the original authors proposing this idea [12].

No-sleep boundary condition is achieved by implementing a bounce-back algorithm on the links [2]. This means that incoming particle portions are reflected back towards the nodes they came from (Fig. 3). In other words:

$$f_6 = f_8 \;\;,\;\; f_2 = f_4 \;\;,\;\; f_5 = f_7 \quad (13)$$

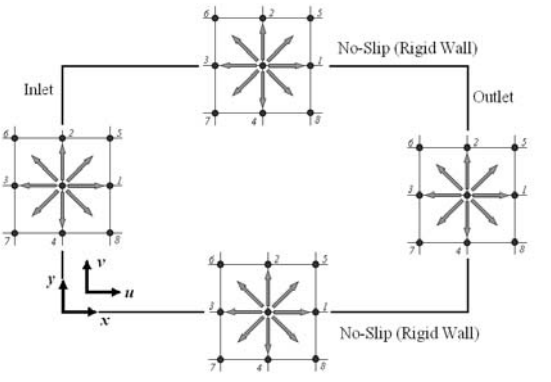

Fig. 3 Physical boundaries of the solution domain and lattice model on typical boundaries

4 SIMULATION RESULTS

The computer code with the cell-centered FV-LBM has been used to simulate plane Poiseuille flow and sudden expansion flow. The results are presented and discussed in this section.

Plane Poiseuille Flow:

This is a pressure-driven flow in a duct with flat parallel walls. At a large upstream distance from the inlet the velocity distribution is assumed to be uniform and parabolic over the width of the channel (Fig. 3). We assume that the velocity in the inlet section is uniformly distributed over its width, 2*a*, and its magnitude is U_{ave}. The Reynolds number is defined as $\mathrm{Re} = U_{avr} H/\nu$ where *H=2h* is channel height and ν is viscosity.

Owing to viscous friction, boundary layers will be formed on both walls and their width will increase in the downstream direction (developing region). The result velocity profile will consist of two boundary layer profiles on the two walls joined in the centre by a line of constant velocity. The boundary layers develop with increasing *x* until they reach the centerline. The flow is then said to be hydro-dynamically fully developed. The analytical solution of flow shows that the velocity profile gradually changes to a parabolic profile at the fully developed region [13]. This profile is defined as following:

$$u(y) = U_{\max}\left(1 - \left(y/h\right)^2\right) \quad (14)$$

Where

$$U_{\max} = \frac{h^2}{8\mu} \cdot \frac{dp}{dx} = 1.5 U_{avr} \quad (15)$$

Once the flow is fully developed the velocity profile does not vary in the flow direction. In fact in this region the pressure gradient and the shear stress in the flow are in balance. The length of the duct between the start and the point where the fully developed flow begins is called the developing length.

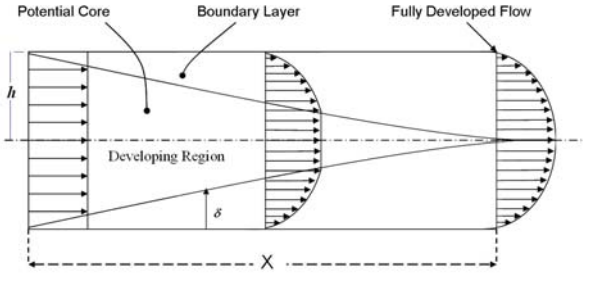

Fig. 4 Schematic of Plane poiseuille flow

Fig. 5 shows a part of the computational domain and velocity vectors in which the lattice Boltzmann equation for the incompressible laminar duct flow is solved. The results of the simulation display essentially laminar growth at the low Reynolds numbers.

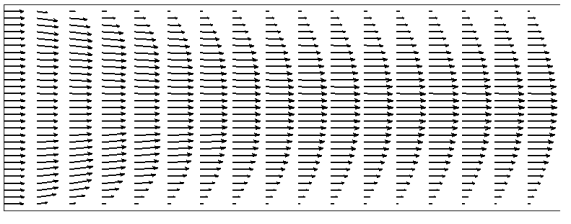

Fig. 5 Velocity vectors of plane poiseuille flow at Re=29

Fig. 6 is a plot of the normalized streamwise velocity profiles at different streamwise locations. The velocities and lengths are normalized by the flow maximum velocity and the channel height, respectively. What is apparent from Fig. 6 is a uniform velocity profile entering at the inlet boundary and then gradually evolving to a velocity profile that is much smoother and, in fact, is parabolic.

In fluid dynamics, the Darcy–Weisbach equation is a phenomenological equation, which relates the head loss or pressure loss due to friction along a given length of pipe or open duct to the average velocity of the fluid flow. This equation contains a dimensionless friction factor, known as the Darcy friction factor [13]. The Darcy friction factor for laminar plane Poiseuille flow is given by the following formula:

$$\lambda = 24/\mathrm{Re}_h \tag{16}$$

Where $\mathrm{Re}_h = U_{ave}.h/v$. Note that the above equation is valid only for fully developed region. The Darcy friction factor is also known as the Moody friction factor and is four times larger than the Fanning or skin friction factor (i.e $\lambda = 4C_f$).

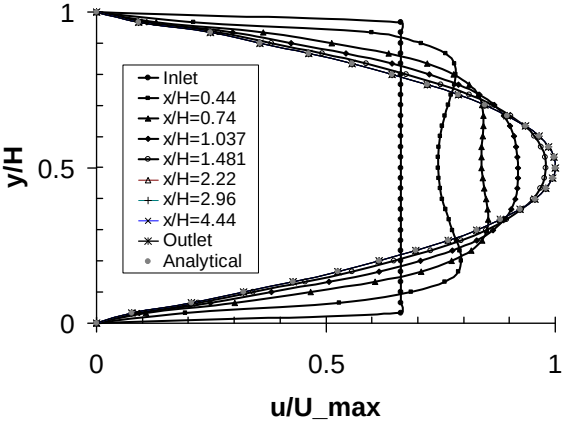

Fig. 6 Streamwise velocity profiles for plane poiseuille flow at different locations and Re=29

Fig. 7 shows the distribution of Darcy friction at Re=29. One can see that the graph is approached to value $24/\mathrm{Re}_h = 0.827$ at fully developed region. The relative error is less than 1.7% which demonstrates that the present scheme predicts accurately the friction distribution along an open channel flow.

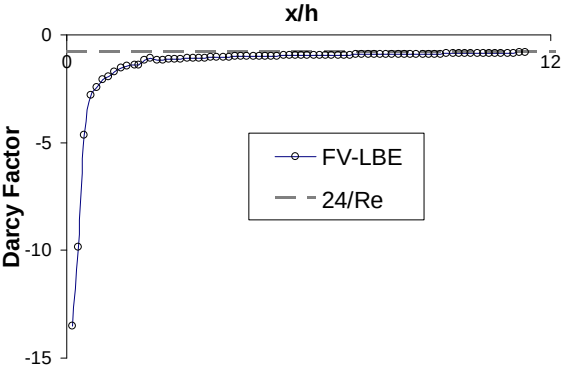

Fig. 7 Darcy friction distribution at Re=29 along plane Poiseuille flow

Channel with a Sudden Expansion:

Incompressible laminar flow in a symmetric plane sudden expansion is a classical fluid flow problem which admits multiple solutions. This fact has been demonstrated both numerically and experimentally by several authors. For Reynolds numbers less than a

certain critical value, the flow in the sudden expansion is symmetric with two equal sized eddies whose length increases linearly with Reynolds number. For Reynolds numbers higher than the critical value, the flow undergoes a symmetry-breaking pitchfork bifurcation rendering the symmetric solution unstable [15-17].

Fig. 8 shows a schematic two-dimensional plot of the flow channel in the experiment. The expansion ratio and the Reynolds number are defined as ER=*H*/*h*=3 and $\mathrm{Re} = U_{\max} h / 2\nu$ respectively. At the entrance, a parabolic velocity profile is enforced. The initial conditions for the velocity field are set to be asymmetric with respect to the symmetric *x*-axis of the channel, $\bar{u}_{y>0} = 0.01$, $\bar{u}_{y<0} = 0$ and $\bar{v} = 0$. The asymmetry of the initial condition determines the branch taken by the asymmetric final state.

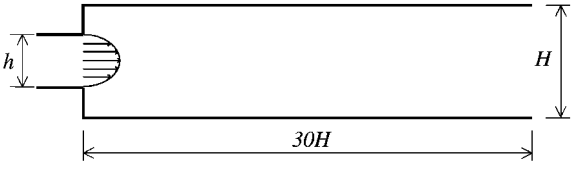

Fig. 8 Schematic of the sudden expansion channel flow

The velocity vectors and streamline contours plot for Re=26 are depicted in Fig. 9. At this Reynolds number, two same recirculation regions form downstream of the expansion.

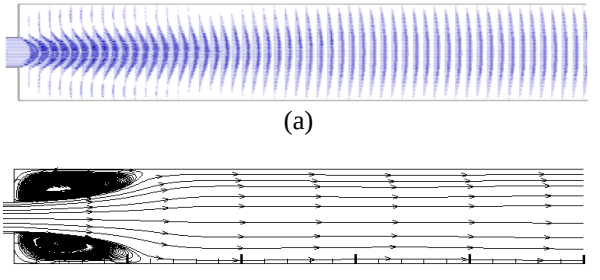

(a)

(b)

Fig. 9 a) Velocity vectors and b) Streamline contours for the sudden expansion channel flow at Re=26

Fig. 10 is a plot of the streamwise velocity profiles, compared at three streamwise locations at Re=26. Good agreement between experimental and numerical results is shown in Fig. 10. One can see that the velocity profile gradually evolving to a fully developed profile by getting away from the inlet.

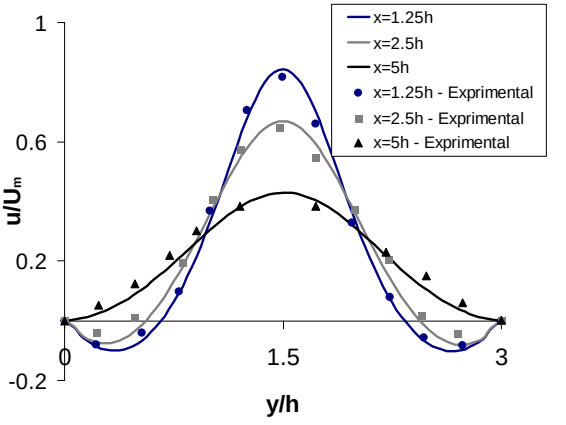

Fig. 10 Velocity profiles at different streamwise locations comparison to experimental data [15]

Early experiments showed that a transition phenomenon from symmetric to asymmetric steady state occurred as the Reynolds number was increased to value above critical Reynolds number [15-17]. In other words, the symmetric flow lost stability to one of a pair of steady asymmetric solutions, with either the upper or lower circulation region becoming longer. Fig. 11 shows velocity vectors and streamline contours for Re=80 compared with experimental results of Fearn et al. [15].

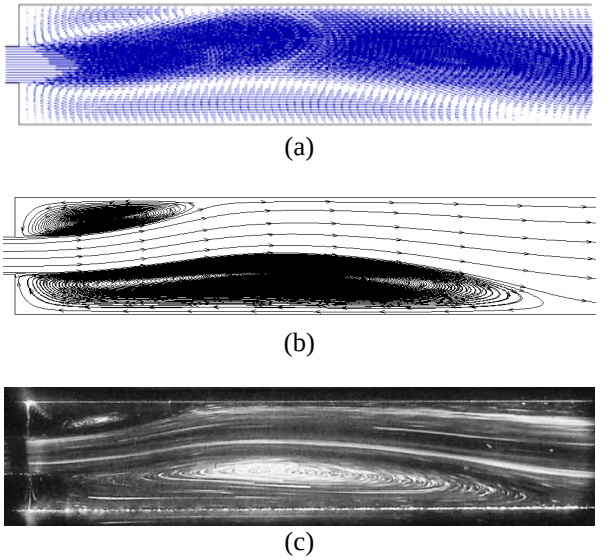

(a)

(b)

(c)

Fig. 11 a) Velocity vectors, b) Streamline contours and c) Experimental results for the sudden expansion channel flow at Re=80

Now, we evaluate the skin friction distributions in the main channel for different Reynolds numbers. The skin friction is defined as following:

$$C_f = \tau_w / 0.5\rho U_{ave}^2 \quad (17)$$

Where τ_w is the wall shear stress and ρ is the fluid density. Skin friction distributions in the downstream channel of ER=3 are given in Fig. 12.

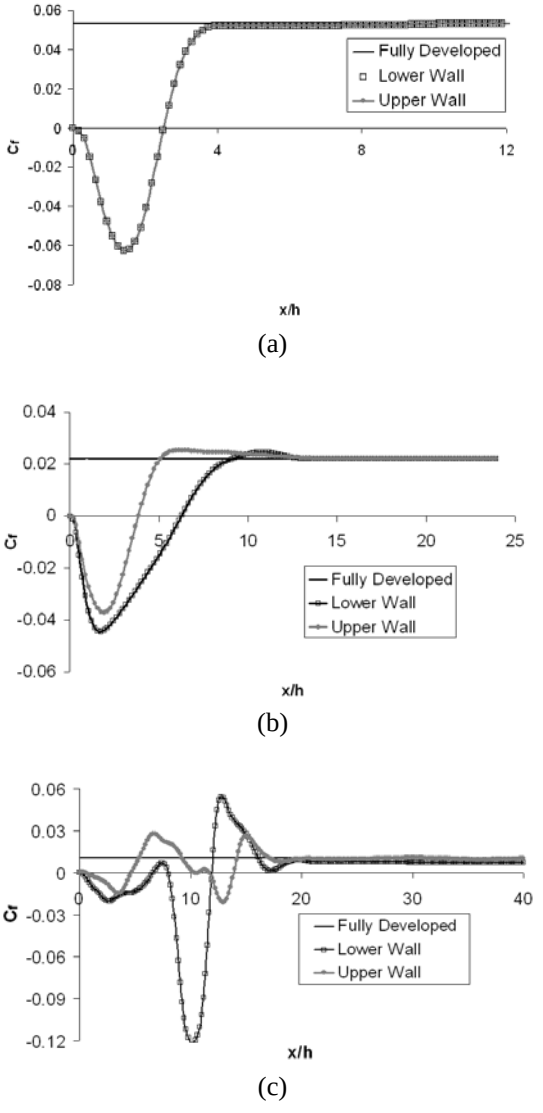

Fig. 12 Skin friction distributions for ER=3 at a) Re=25, b) Re=60 and c) Re=80

The skin friction distribution reveals that the flow regains symmetry after some redeveloping length downstream of the expansion plane, at which the skin friction attains its fully developed value of $C_f = (12/\mathrm{Re}) \times (h/H)^2$ [18]. It is apparent that skin friction values, in the redeveloping region, exhibit major departures from their fully developed value.

5 CONCLUSION

A cell centered finite volume formulation of LBM has been presented on D2Q9 lattice to study skin friction distributions of channel flows. Also, consistent boundary conditions based on cell centered finite volume are addressed. Using the present method, we simulate plane poiseuille flow and sudden expansion flow. A good agreement between present results and analytical or experimental solutions is observed. It is shown that the Darcy friction distribution in plane poiseuille flow is approached to $24/\mathrm{Re}_h$ at fully developed region whereas the skin friction distribution in sudden expansion channel flow is attained to $C_f = (12/\mathrm{Re}) \times (h/H)^2$ at fully developed region.

ACKNOWLEDGMENTS

The authors would like to thank officials in Science and Research Branch, Islamic Azad University, Fars for providing financial support for this research.

REFERENCES

[1] Benzi, R., Succi, S., and Vergassola, M., "The Lattice Boltzmann Equation: Theory and Applications", Physics Reports, Vol. 222, No. 3, 1992, pp. 145-197.

[2] Succi, S., "The Lattice Boltzmann Equation for Fluid Dynamics and Beyond", Clarendon, Oxford, 2001.

[3] Gladrow, D. A., "Lattice-Gas Cellular Automata and Lattice Boltzmann Models: An Introduction. Lecture Notes in Mathematics", Springer, Berlin, 2000.

[4] Nannelli, F., and Succi, S., "The Lattice Boltzmann Equation on Irregular Lattices", Journal of Statistical Physics, Vol. 68, 1992, pp. 401-407.

[5] Bhaumik, S. K., and Lakshmisha, K. N., "Lattice Boltzmann Simulation of Lid-Driven Swirling Flow in Confined Cylindrical Cavity", Computers and Fluids, Vol. 36, 2007, pp. 1163-1173.

[6] Ubertini, S., Succi, S., and Bella, G., "Lattice Boltzmann Schemes Without Coordinates", Philosophical Transactions of the Royal Society A., Vol. 362, 2004, pp. 1763-1771.

[7] Zarghami, A., Maghrebi, M. J., Ubertini, S., and Succi, S., "Modeling of Bifurcation Phenomena in Suddenly Expanded Flows with a New Finite Volume Lattice Boltzmann Method", International Journal of Modern Physics C, Vol. 22, 2011, pp. 977-1003.

[8] Bhatnagar, P. L., Gross, E. P., and Krook, M., "A Model for Collision Processes in Gases, I. Small Amplitude Processes in Charged and Neutralone-Component System", Physics Review, Vol. 94, 1954, pp. 511-525.

[9] Ubertini, S., and Succi, S., "Recent Advances of Lattice Boltzmann Techniques on Unstructured Grids", Progress in Computational Fluid Dynamics, Vol. 5, 2005, pp. 85-96.

[10] Stiebler, M. J., and Krafczyk, M., "An Upwind Discretization Scheme for the Finite Volume Lattice Boltzmann Method", Computers and Fluids, Vol. 35, 2006, pp. 814-819.
[11] Zarghami, A., Maghrebi, M. J., Ghasemi, J., and Ubertini, S., "Finite Volume Lattice Boltzmann Formulation with Improved Stability", Communications in Computational Physics, Vol. 12, 2012, pp. 42-64.
[12] Zou, Q., and He, X., "On Pressure and Velocity Boundary Conditions for the Lattice Boltzmann BGK Model", Physics of Fluids, Vol. 9, 1997, pp. 1591-1598.
[13] Schlichting, H., "Boundary Layer Theory", Springer-Verlag, 2005.
[14] Chen, R. Y., "Flow in the entrance region at low Reynolds numbers", Journal of Fluid Engineering, Vol. 95, 1973, pp. 153-158.
[15] Fearn, R. M., Mullin, T., and Cliffe, K. A., "Nonlinear flow phenomena in a symmetric sudden expansion", Journal of Fluid Mechanics, Vol. 211, 1990, pp. 595-608.
[16] Hawa, T., and Rusak, Z., "Viscous flow in a slightly asymmetric channel with a sudden expansion", Physics of Fluids, Vol. 12, 2000, pp. 2257-2264.
[17] Battaglia, F., Tavener, S. J., Kulkarni, A. K., and Merkle, C. L., "Bifurcation of low Reynolds number flows in symmetric channels", AIAA Journal, Vol. 35, 1997, pp. 99-105.
[18] Wahba, M., "Iterative solvers and inflow boundary conditions for plane sudden expansion flows", Applied Mathematical Modeling, Vol. 31, 2007, pp. 2553-2563.